



The Use of Satellite Data to Quantify Thermal Effluent Impacts

J. F. Mustard^a, M. A. Carney^b and A. Sen^c

Department of Geological Sciences, Box 1846, Brown University, Providence, RI 02912, U.S.A.

Received 11 December 1998 and accepted in revised form 19 April 1999

Thermal effluent from a large coal-fired electric generating facility located on Mt. Hope Bay in the Narragansett Bay (Rhode Island, U.S.A.) has been implicated in a large decline in fish populations in this region. Detailed information on the spatial and temporal properties of this thermal input (approximately 5 million m³ day⁻¹ of thermal effluent 7 °C above ambient) is, however, lacking. In this paper it is shown that the spatial extent and magnitude of the thermal impacts can be quantitatively determined by exploiting the strengths of remotely sensed data. Seasonal trends of surface temperature in the Narragansett Bay estuary were derived from a composite of 14 thermal infrared satellite images (Landsat TM Band 6) with a spatial resolution of 120 m. The derived temperatures were validated against independent measures of surface temperature for a number of sites within the bay, and it was shown that the satellite measures were within 1 °C of the *in situ* temperatures. Relationships among thermal properties and physical characteristics were identified through a comparison of the seasonal temperature patterns of 12 regions within the bay. As expected, depth was the primary factor in determining the magnitude of seasonal temperature variation in the estuary, while advective exchange with the coast ocean was the second most important factor. Although the behaviour of Mount Hope Bay was significantly correlated with the other upper estuarine regions, the bay did not experience autumn cooling, which is characteristic of upper estuarine waters. From late summer through to autumn, the average temperature difference between Mount Hope Bay and Upper Narragansett Bay was 0.8 °C, which can be attributed to warming from the thermal effluent of the Brayton Point Power Station in Mount Hope Bay. An unsupervised (statistical) classification of temperature as a function of season revealed the natural boundaries between areas with different seasonal temperature signals, and statistically identified Mount Hope Bay as a unique area in the upper estuary which had anomalously high temperatures throughout the year. Among the scenes included in the unsupervised analysis, Mount Hope Bay was on average 0.8 °C warmer than the rest of the upper estuary, and the total area affected is 36 km². © 1999 Academic Press

Keywords: remote sensing; thermal effluent; environmental impacts; Narragansett Bay RI

Introduction

The highly dynamic environment of an estuary presents significant challenges to the characterization (e.g. scope and magnitude) of environmental impacts of effluent. In this paper, an approach is presented that allows a quantitative assessment of the environmental impact of thermal effluent in an estuary. In general, such an assessment requires both a comprehensive understanding of the natural thermal behaviour of a given system and measurements with sufficient precision, spatial coverage, and temporal frequency to constrain the problem. A widely used approach to detect environmental impact is the before–after; control–impact (BACI) method

(Stewart-Oaten *et al.*, 1986). In this approach a key variable is analysed in both an allegedly impacted site and a control site or sites. The variable must exhibit a statistically significant change in the impacted site relative to the control site, after the effects of a defined disturbance (Underwood, 1993).

In many situations, however, pre-impact data are either not available or are insufficient to rationally test the impact hypothesis. For example, water temperatures in estuaries are extremely dynamic and vary with tides, diurnal heating and cooling, weather systems, as well as seasonally. To apply the BACI method, several impact data records would need to be compared with an equal or greater number of control sites. The data records would need to be of sufficient temporal resolution and length such that the highly variable influences of tides, weather, seasons, etc. could be removed. Furthermore, statistically significant differences in point measurements are difficult to establish in such complex and dynamic environments due to

^aCorresponding author. Tel: 401 863 1264; fax: 401 863 3978; e-mail: John_Mustard@brown.edu

^bCurrently at: Science Applications International Corporation, 4501 Daly Dr. Suite 400, Chantilly, VA 20151, U.S.A.

^cCurrently at: Abt Associates Inc., 55 Wheeler St, Cambridge, MA 02138, U.S.A.

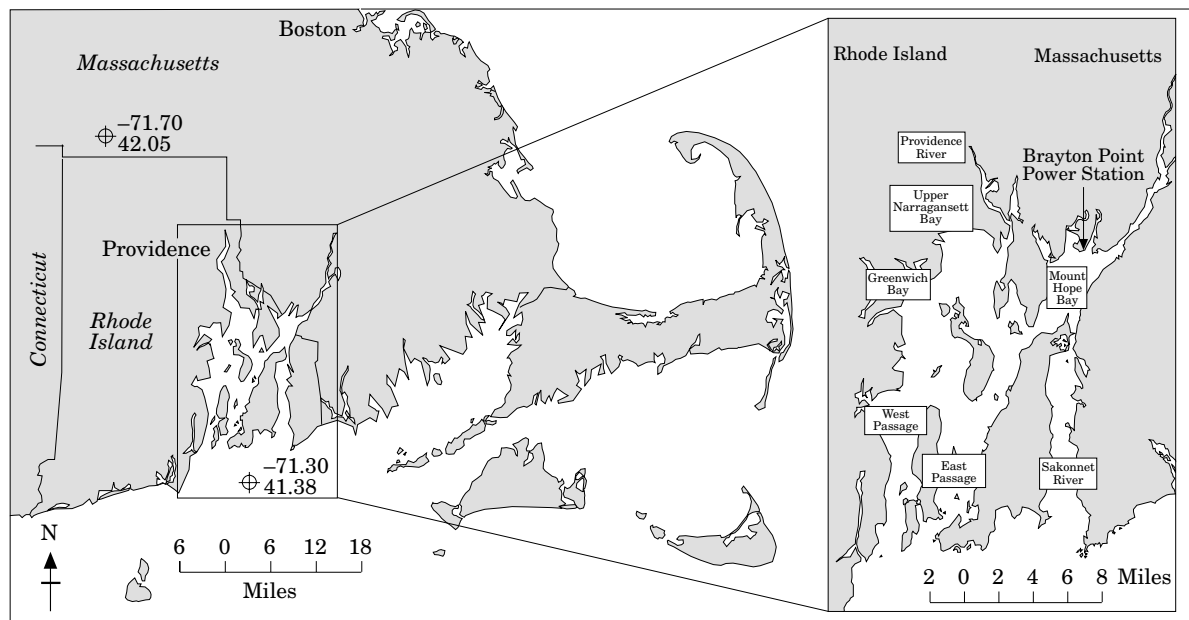


FIGURE 1. Location of the study area. Narragansett Bay is largely within the state of Rhode Island, although Mount Hope Bay and the Brayton Point Power Station are within the state of Massachusetts.

uncertainties in linking measurements across larger spatial scales. Needless to say, long-term, high-resolution, properly sited data sets for such purposes are rare to non-existent.

When pre-impact data are unavailable or insufficient to constrain the problem, a substitute site, similar in physical characteristics to the allegedly impacted site, can be used instead. This approach, known as Space For Time (SFT) substitution (Hargrove *et al.*, 1992; Hamburg, 1984) has been demonstrated to be particularly valuable in understanding landscape-scale processes that occur over long periods of time (Hurlbert, 1984; Hargrove *et al.*, 1992). Clearly, the limitations of the SFT approach arise when the control and impacted sites are not functionally comparable, or if factors different than the hypothesized environmental perturbation have contributed to fundamental changes in the processes operating in the given areas.

In this paper, it is demonstrated that satellite measurements of surface temperature provide an ideal tool to apply the SFT approach in a dynamic estuarine environment. *In situ* data records are typically incomplete and cannot be confidently linked across the spatial scales necessary to statistically test the impact hypothesis. In contrast, satellite observations of surface temperature provide a nearly instantaneous and spatially continuous measurement for many thousands of uniform grid cells across a given area. Though the precision (0.5 °C) and uncertainty of satellite measurements do not presently match *in situ*

instruments, the numerous measurements across large spatial scales compensate for this and allows an effectively high precision.

Study area and definition of the problem

The Narragansett Bay estuary runs northward from the coast of Rhode Island (U.S.A.) (Figure 1), and has a drainage area of 4660 km² (Kremer & Nixon, 1978). Its 2.6×10^9 m³ of water are spread over an area of almost 350 km², with a mean depth of 7.8 m (Chinman & Nixon, 1985). The mean tidal prism is much greater than the mean volume of river flow into the bay during an equivalent period of time, so that the estuary is generally well mixed, although occasionally stratified (measured by salinity gradients) in the upper bay (Kremer & Nixon, 1978). The semi-diurnal tide ranges from 0.8 to 1.6 m (Chinman & Nixon, 1985), but the prevailing winds, north-west during the winter and south-west during the summer, frequently dominate short-term circulation patterns (Kremer & Nixon, 1978). Water temperatures throughout the year range from below freezing up to the mid-20s (°C) and the annual water temperature cycle tends to lag solar radiation by about 40 days (Kremer & Nixon, 1978).

The Narragansett Bay ecosystem is phytoplankton based and usually experiences a bay-wide winter-early spring bloom, several localized short-term blooms throughout the summer and a late summer bay-wide bloom (Kremer & Nixon, 1978). The bay is inhabited

by many commercially important fish species, is an important breeding and nursery area for fish and the benthos is dominated by clams which are harvested in limited areas. The land surrounding the estuary is heavily populated and the estuary receives significant volumes of industrial and municipal effluents. Although the overall quality of the water in the estuary has improved dramatically over the last several decades, Gibson (1996) identified a strong, temporal correlation between fish abundance and changes in the operation of a power plant located on the upper reaches of Narragansett Bay. Specifically, the onset of a major decline in aggregate fin fish stocks and species diversity over the last decade was significantly correlated with a 50% increase in the volume of effluent discharged from the Brayton Point Power Station (BPPS) in 1985.

The BPPS is the largest fossil fuel power plant in the north-east United States. This coal-fired electric generating facility is located on Mount Hope Bay in the Narragansett Bay estuary (Figure 1) and releases approximately 5 million $\text{m}^3 \text{day}^{-1}$ of thermal effluent ($\approx 60 \text{ m}^3 \text{s}^{-1}$). The water, used for cooling, is extracted from and returned to the estuary with a typical temperature rise of 7–10 °C over the ambient temperature of the input water. Concerns have been raised about the long term impacts of the thermal effluent on the Mount Hope Bay ecosystem such as the effects on dissolved oxygen and reproductive success of organisms (Jeffries, 1994; Lin & Regier, 1995) as well as the possibility that it may be a factor in the decline of fish stocks in this bay over the past 15 years (Gibson, 1996). However, detailed information on the fate of the thermal effluent and its spatial and temporal properties over short and long time periods are lacking. This essential information is required in order to objectively assess the overall impact of the thermal effluent on diurnal and seasonal time scales and to integrate this into a more detailed understanding of the local ecology.

Temperature affects organisms through direct physiological mechanisms. All organisms have a certain tolerable temperature range, above which prolonged exposure is lethal. Within this acceptable temperature range, metabolism, growth rates, reproduction and recruitment success vary widely. In cold-blooded marine organisms, warmer ambient temperatures increase metabolic rates and related processes, such as feeding efficiency. Growth and development rates usually increase with temperature, up to a threshold, beyond which excess energy is required for survival, and rates decline precipitously. Temperature variations are used as reproductive cues for many populations, including several Narragansett

Bay fish species (Dixon, 1991). Increases in bacterial abundance with temperature (Valiela, 1995), further compound the community effects of reduced dissolved oxygen and nutrient concentrations in warm water (Paine, 1993).

All of these temperature-related responses affect different species and the repercussions for ecosystem dynamics depend upon food web interactions. Despite lack of a clear understanding of the mechanisms at work, significant warming of coastal marine systems has been documented to have substantial and sometimes unpredictable impacts upon community composition and structure (Tissot *et al.*, 1991). Thus, a detailed understanding of estuarine thermal processes and anthropogenic impacts upon them are vital to the successful management of coastal ecosystems and fisheries.

In this analysis it is sought to establish the magnitude and scope of the impact of thermal effluent from the BPPS in the Narragansett Bay estuary and Mount Hope Bay in particular. Because there is insufficient *in situ* thermal data of the Narragansett and Mount Hope bays acquired prior to the construction of the power plant, prior to the 1985 modifications, and even being acquired today, a different set of observations is required to make this assessment. Satellite measurements of surface temperature provide a unique perspective on this problem. Because the data are acquired essentially instantaneously over the entire study region, it is possible to directly compare the thermal characteristics of Mount Hope Bay in the context of the surrounding system at the time of the measurement. Also, since the data are acquired in an image format, it is possible to establish patterns of thermal properties across large spatial scales. Finally, since these satellite data have been acquired with some regularity since 1981, repeated measurements of the system can be utilized to establish seasonal and tidal variations.

Methods

Landsat thematic mapper data

Since 1981, the Landsat Thematic Mapper (TM) series instruments have acquired multispectral images of the surface of the Earth from an orbit of 700 km. Of importance to this investigation, the TM sensor includes one thermal infrared channel that covers the wavelength region 10.4–12.5 μm from which an estimate of surface temperature can be derived (see below). The spatial resolution of each picture element (pixel) on the surface in the thermal channel is 120 m \times 120 m, or slightly more than 1.4 hectares.

TABLE 1. Landsat scene acquisition

Date	Tidal Stage
01/01/1992	72% ebb
20/02/1987	60% flood
02/05/1984	23% ebb
03/07/1989	40% ebb
09/08/1985	44% flood
15/08/1993	82% ebb
06/09/1995	82% ebb
07/09/1984	70% ebb
13/09/1986	17% flood
16/09/1987	33% flood
27/09/1991	98% flood
28/10/1985	44% ebb
31/10/1986	67% ebb
26/11/1984	96% flood

From its sun synchronous orbit, this sensor has the opportunity to re-visit a specific target every 16 days. However, the frequency of actual data collected is far less than this due to obscuration by clouds and scheduling of spacecraft data handling resources. Although other sensors have more frequent observations (e.g. the Advanced Very High Resolution Radiometer acquires thermal data twice a day and these sensors have been in operation since 1979), they lack the requisite spatial resolution to resolve the thermal properties of specific regions within Narragansett Bay.

Narragansett Bay is within Landsat TM Path 13, Row 31. For this investigation, the Landsat TM archives were searched at the United State Geological Survey's Earth Resources Observations Systems (EROS) data centre for any acquisitions of Path 13, Row 31 that met an initial requirement of <20% cloud cover. This resulted in 35 listed acquisitions from 1981 to 1996. Unfortunately, many of the scenes had more cloud cover than estimated in the data base, or were no longer in the archive. In addition, a remarkable series of eight scenes, well distributed across the year 1988 was acquired. However, there were no useable data acquired in the thermal channel for any of these scenes. Eliminating scenes with no useful data due to obscuration by clouds and other factors, a final total of 14 scenes reasonably well distributed across the calendar year was obtained (Table 1, Figure 2).

Temperature derivation

Radiance measurements from band six of the Landsat Thematic Mapper (wavelength $\times 10.4$ – $12.5 \mu\text{m}$) were used to derive surface temperatures by applying a form of Planck's Black Body Equation, which defines the relationship between the radiance emitted from an

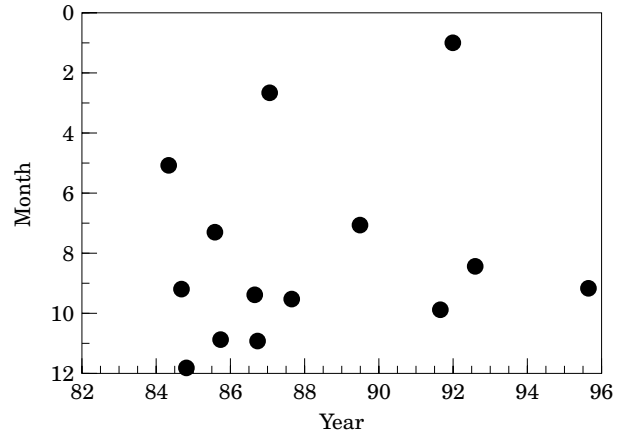


FIGURE 2. Distribution of the 14 Landsat TM scenes used in this analysis as a function of year (horizontal axis) and month (vertical axis).

object at a certain wavelength and its absolute temperature. First, the image digital number (DN) values were converted to at-sensor radiance by applying the gain and bias of the detectors where:

$$R_u = a(\text{DN}) + \beta$$

where:

R_u = uncorrected spectral radiance in $\text{mW cm}^{-2} \text{Sr}^{-1} \mu\text{m}^{-1}$

$a = 0.005632 \text{ mW cm}^{-2} \text{Sr}^{-1} \mu\text{m}^{-1} \text{DN}^{-1}$

$\beta = 0.1238 \text{ mW cm}^{-2} \text{Sr}^{-1} \mu\text{m}^{-1}$

Radiance was then converted to a black body temperature (Gibbons *et al.*, 1989):

$$T_u = \frac{K_2}{\ln \left[\frac{K_1}{R_u} + 1 \right]}$$

where:

T_u = black body temperature in K

$K_2 = 1260.56 \text{ K}$

$K_1 = 60.776 \text{ mW cm}^{-2} \text{Sr}^{-1} \mu\text{m}^{-1}$

Because water is not a perfect black body (or a perfect emitter), a correction was made using the emissivity of water (the ratio between the radiance of a particular 'grey body' and that of a black body at the same temperature) (Avery & Berlin, 1992):

$$T_k = T_u / E^{1/4}$$

where:

E = emissivity of water = 0.986 (Gibbons *et al.*, 1989)

T_k = kinetic temperature in K

Low atmospheric transmissivity can introduce some error into deriving surface temperature from satellites, as atmospheric constituents (especially water vapour) absorb radiation emitted from the surface, thus reducing the amount of radiation which actually reaches the sensor. The atmosphere also emits some radiation due to its own internal heat, in turn increasing at-satellite radiance. The net effect will typically reduce the magnitude of the at-sensor radiance compared to the surface radiance, as well as the contrast or dynamic range.

The accuracy and precision of deriving surface temperatures from Landsat TM band six data have been assessed by Schneider and Mauser (1996), who employed a full atmospheric model to convert at-satellite radiance to an accurate measure of water leaving radiance (and thus water temperature) of a lake in Germany for which extensive *in situ* water temperature data were available. On average (in 31 images), atmospheric correction increased satellite derived temperatures by 1.33 K. Thus, we may expect to slightly underestimate temperatures when corrections are not made, although the exact error is dependent upon specific atmospheric conditions. Atmospheric corrections also increased spacing, or the temperature step associated with one DN step, from 0.47 K DN⁻¹ to 0.63 K DN⁻¹. Therefore, temperature differences may also be slightly underestimated. For their data, Schneider and Mauser (1996) estimated the average change in temperature difference was +0.16 D DN⁻¹.

A critical factor to consider is the relationship between the remotely sensed surface layer and the bulk water properties. Here the bulk water temperatures are defined to include the water above the thermocline, which in a well-mixed estuary may extend to the bottom. All of the energy exchanges between water and air take place within a very thin surface skin layer, the layer that is sensed remotely. Due to evaporative cooling in the surface layer, this temperature is typically cooler than the bulk water temperature, though sea state, wind speed, and diurnal energy fluxes all affect the relationship. The exact nature of this relationship is complicated and has been studied by numerous investigators. Yokoyama *et al.* (1995) showed that under typical coastal ocean conditions, thermal gradients from the surface to 2 metres were weak to absent and they concluded that the skin temperature was a reasonable estimate of the bulk temperature. They did note that under extremely calm conditions, strong thermal gradients developed in the near surface, sometimes exceeding several °C. However, the time of maximum divergence was typically between 12:00 and 16:00 h

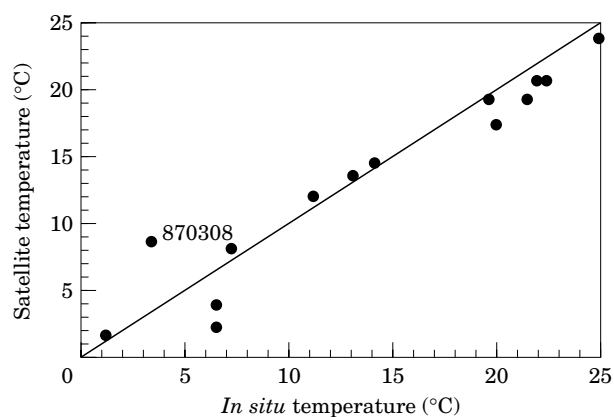


FIGURE 3. Satellite derived surface temperatures compared to *in situ* water temperatures. The solid line represents the 1:1 relationship.

local time. Schneider and Mauser (1996) investigated the relationship between radiometric measurements of surface temperatures and bulk water temperature over many diurnal cycles. On average, the temperature difference was found to be at a minimum (0.1 K) between 09:00 and 11:00 h, the standard crossing time of the Landsat satellites. On the basis of these and other studies it is concluded that remotely measured skin temperatures are representative of bulk water temperature below the surface.

As a test of this relationship, temperatures derived from the fourteen satellite images were compared to *in situ* measurements to assess the level of accuracy of the calculated temperatures for this study (Figure 3). In cases where an *in situ* measurement was available for the day of the overflight, a direct comparison could be made. Because these situations were rare, any *in situ* data available within one day of the overflight were used as estimates. When measurements were not available within one day, temperatures were linearly interpolated from measurements within 3 days before and after the scene date.

Satellite-derived temperatures were all within 3 °C, and many within 1 °C of *in situ* measurements. All of the other differences greater than 1 °C were satellite underestimates probably resulted from atmospheric interference. The derived temperatures were used to compare the general seasonal water temperature trend in the satellite images to actual trends observed through years of *in situ* monitoring. The seasonal composite created from fourteen satellite images which actually span over twelve years (Figure 2) was found to be an appropriate representation of the general seasonal trends observed over the long term (Figure 4).

While the level of accuracy of the remotely acquired data is important, the goal of this investigation is to

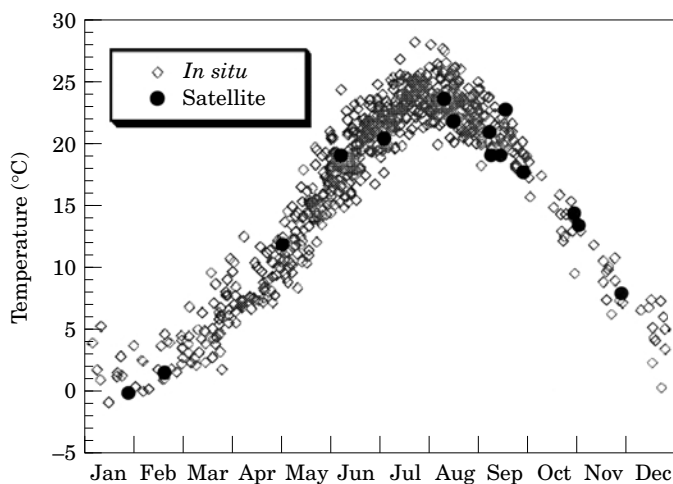


FIGURE 4. Seasonal composite of satellite derived temperatures, covering the period 1984–1996 and a 20-year record of temperatures from one station in Mount Hope Bay. The satellite temperatures track well within the range of the *in situ* records.

determine if the thermal effluent has a measurable impact on water temperatures beyond the immediate area of the effluent discharge point. For this purpose we can take advantage of the high precision of the remote measurements ($0.5\text{ }^{\circ}\text{C}$) and image format of the data and analyse the temperature of each area relative to a baseline, thus eliminating the uncertainty involved in deriving exact temperatures. For a baseline the mean temperature of the entire Narragansett Bay estuary was chosen. Deviations of specific areas from the estuary mean were generally within the range of $\pm 5\text{ DN}$ or $\pm 2.5\text{ }^{\circ}\text{C}$. Given the fact that atmospheric effects tend to increase the temperature/DN relationship, this range in temperatures may be an underestimate of the order of $0.8\text{ }^{\circ}\text{C}$, for the largest deviations. A fundamental assumption of this approach is that the atmosphere does not vary significantly across the scene ($60 \times 90\text{ km}$). This assumption will be valid under clear sky conditions. However the presence of clouds or fog may introduce non-uniform variations and thus scenes with significant clouds or fog were removed from the study.

Regional classification of Narragansett Bay

To facilitate studies of the physical characteristics of Narragansett Bay, Chinman and Nixon (1985) divided the estuary into a series of distinct segments related to basin bathymetry and circulation patterns and defined the depth, area, and volume of each of these segments (Table 2). Based upon this breakdown as well as observations of overall temperature patterns in the estuary, 12 study areas within Narragansett Bay were defined (Figure 5), in order to investigate spatial

variations in seasonal temperature trends. The ‘regional classification’ consisted of categorizing the behaviour of these pre-defined regions relative to the system as a whole. Four areas were defined in the upper estuary (Greenwich Bay, Providence River, Upper Narragansett Bay, Mount Hope Bay) and the West Passage, East Passage, and Sakonnet Rivers were each divided into two or three sections so that estuary-to-ocean gradients could be detected where present. The known physical characteristics for each area (Table 2) provide a context for comparison of their seasonal temperature patterns. Temperature data were also extracted from two inland water bodies and the coastal ocean (Figure 5) for comparison to estuarine characteristics. The temperature of the estuary as a whole was defined as the mean of the combination of all of the Narragansett Bay study areas.

Surface temperature signals were produced by extracting the mean temperature from each study area and calculating its temperature difference from the Narragansett Bay mean for each scene ((regional mean) – (Narr. Bay mean)). Correlation coefficients among each of the normalized seasonal temperature signals were used as a means for classifying the estuary in terms of its thermal properties (Table 3). Three natural groups are defined from the correlations in Table 3, where each group exhibits a positive correlation among its members and a negative correlation with the other groups.

Unsupervised classification of Narragansett Bay

The regional approach discussed above incorporated knowledge of the estuary’s morphology and

TABLE 2. Physical characteristics of regions within Narragansett Bay (Chinman & Nixon, 1985)

Segment	PRR	UNB	MHB	GRB	UWP	LWP	UEP	MEP	LEP	SR
Area (km ²)	21.28	43.29	35.2	11.64	77.92	17.94	23.81	34.34	25.34	50.97
Mean depth (m)	5.21	5.57	5.73	2.11	6.09	8.93	7.33	13.96	18.72	6.5
Mean low water volume (m ³ × 10 ⁶)	110.9	241.3	201.7	24.6	474.5	160.2	174.6	479.4	474.3	331.5
Mean high water volume	137.5	294.1	239.4	38.8	564.9	179.4	202.9	518.2	501.5	386.1
Tidal prism	26.6	52.8	37.7	14.2	90.4	19.2	28.3	38.8	27.2	54.6
Tidal flushing (no. cycles)	4.17	4.57	5.35	1.73	5.25	8.34	6.17	12.36	17.44	6.07
Tidal flushing (days)	2.17	2.38	2.79	0.90	2.73	4.35	3.21	6.44	9.08	3.16
Annual average (m ³ s ⁻¹)										
Fresh water flux	43.22	46.86	30.56	4.01						
Fresh water Flushing (days)	29.7	59.6	76.4	71.0						
Surface Area/volume	0.192	0.179	0.175	0.473	0.164	0.112	0.136	0.072	0.053	0.154

PRR Providence River; UNB, Upper Narragansett Bay; MHB, Mount Hope Bay; GRB, Greenwich Bay; UWP, Upper West Passage; LWP, Lower West Passage; UEP, Upper East Passage; MEP, Middle East Passage; LEP, Lower East Passage; SR, Sakonnet River; MLW, mean low water; MHW, mean high water; FW, fresh water.

circulation patterns to define study areas such that thermal properties could be related to known physical characteristics, i.e. depth, area and volume relationships, and tidal and freshwater flushing. This breakdown was well-suited for gaining an understanding of the seasonal thermal behaviour of different areas of the bay and comparing them to one another in the context of their physical characteristics. However, in treating the estuary as 12 large areas, each with a mean temperature, we fail to maximize the advantages provided by the spatial extent and resolution of remotely sensed data. The large number of data points does give us great confidence that the mean temperature is an accurate representation of the study area, but the process of assigning one value to each pre-defined area may prevent us from observing some important patterns within the data. By pre-defining the study areas, it is assumed that each of these areas behaves as one fairly cohesive system and that this set of study areas is somewhat representative of temperature variations within the estuary. Though these assumptions are valid in the context of a comparison of the properties of different areas, another technique was employed to obtain a more complete view of the estuary's temperature dynamics.

Unsupervised classification is a commonly used technique in the analysis of remotely sensed data (e.g. Jahne, 1991; Foody *et al.*, 1990; Jensen, 1996). It is typically applied to multispectral data of a single date to derive land cover units, but can be readily applied to any multivariate data set. In contrast to the directed, regional classification, unsupervised classification is a completely objective method where statistical relationships among data determine which areas could be treated as cohesive systems. Instead of comparing the averaged seasonal temperature signals of

the selected bay regions, the signals (or vectors) of each pixel are analysed and grouped into statistically categorized classes, thereby dividing the estuary into natural groupings based upon seasonal temperature patterns.

The approach to unsupervised classification that is employed here is a clustering algorithm referred to as the Iterative Self Organizing Data Analysis Technique (ISODATA, Tou & Conzales, 1977; Sabins, 1987; Jain, 1989). As an iterative technique, many passes are made through the data set, successively refining the clustering of the data to achieve the specific constraints imposed on the algorithm or until no further improvement in the clustering is made. The initial characteristics of each class (expressed as a vector, which describes the values of a pixel in all bands, or times, in n-dimensional space) are chosen randomly and then redefined as the classes are formed. Each pixel is placed into the class to which its vector is most similar, and once all of the pixels are classified, a new class vector is defined as the mean vector of all of the pixels in the class. The image is then reclassified, mean vectors recalculated, and the process continues until no significant change occurs between classifications.

Unsupervised classification provides the distinct advantage of objectivity, while allowing some control over the character of the results. The optimum, minimum, and maximum number of classes desired (8, 5, and 14 respectively), the maximum allowable variance within a class (± 10 DN), and the minimum size for a class (999) were all input to shape the analysis. By defining these constraints and a set of computational parameters, the splitting and merging of classes was controlled without making any assumptions about the specific character of each class.

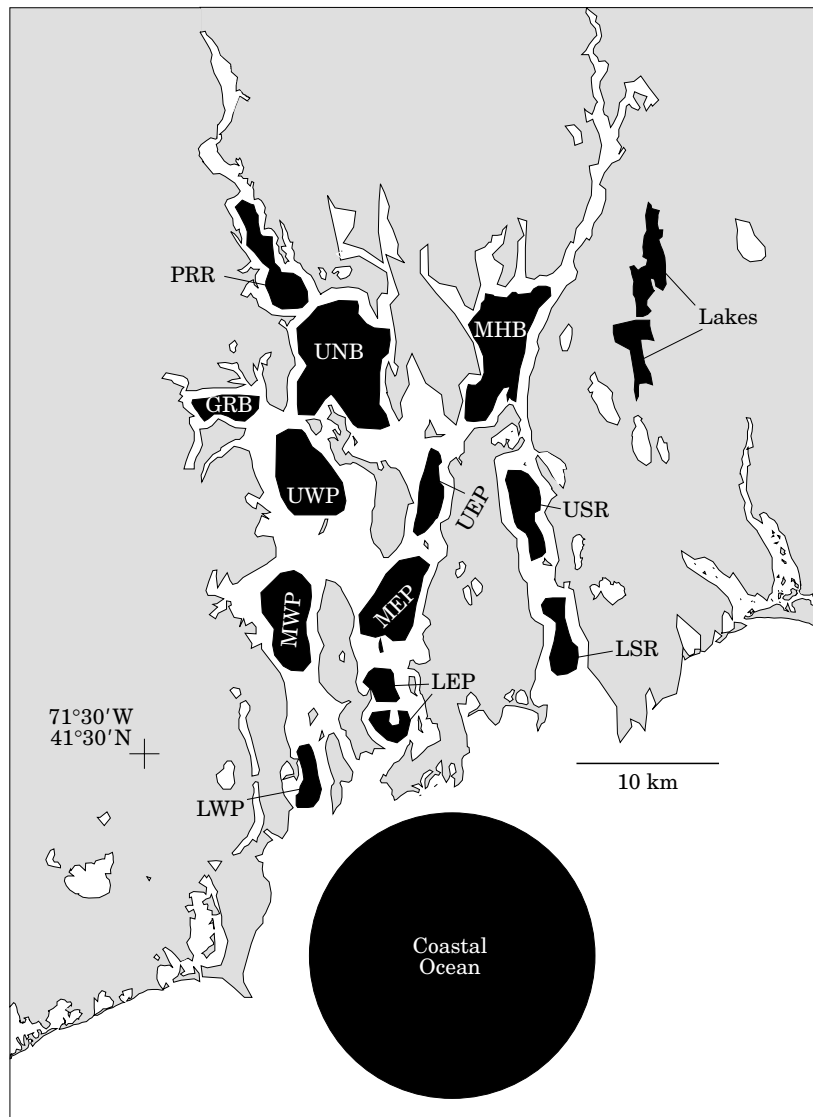


FIGURE 5. Areas from which seasonal temperature signatures were derived for the regional classification analysis. Three letter codes are explained in Table 3.

Eight scenes were selected from the 14 scenes used in this study to perform an unsupervised classification of temperature data. All scenes with any indication of atmospheric interference were removed from the initial set of 14 as well as one scene where ice was present in the bay and a seasonal spread was selected from those remaining. This was to minimize any bias in the results from the large number of September scenes in the full data set.

The water area defined for classification included all of Narragansett Bay and surrounding freshwater bodies, as well as a small part of the coastal ocean. The actual temperature variation within the estuary is very small in comparison to overall seasonal changes, therefore the data were normalized to emphasize tem-

perature variations relative to the estuary mean. The mean DN value was extracted from the defined classification area for each of the seven scenes and the data were normalized using the following formula (which includes adjustments to scale the data within an 8-bit range of 0–255):

$$\text{OUTPUT} = ((\text{INPUT}/\text{MEAN}) - 1) \times 500 + 70$$

The optimal number of classes was set at eight (the range from five to 14), with the goal of identifying large scale differences in seasonal temperature patterns. This range was chosen in an attempt to avoid forming a large number of very small classes which would be difficult to interpret, while at the same time

TABLE 3. Correlations of relative seasonal temperature signals among Narragansett Bay regions

	GRB	MHB	PRR	UNB	USR	UWP	MWP	LWP	UEP	MEP	LEP	LSR
GRB	1	0.86	0.88	0.78	0.26	0.10	-0.55	-0.92	-0.96	-0.99	-0.94	-0.71
MHB		1	0.80	0.48	-0.02	-0.18	-0.47	-0.73	-0.85	-0.83	-0.75	-0.61
PRR			1	0.75	0.02	-0.09	-0.68	-0.81	-0.89	-0.90	-0.81	-0.51
UNB				1	0.40	0.38	-0.81	-0.89	-0.73	-0.84	-0.83	-0.67
USR					1	0.91	-0.91	-0.51	-0.14	-0.32	-0.53	-0.55
UWP						1	-0.18	-0.40	0.00	-0.19	-0.41	-0.56
MWP							1	0.71	0.47	0.62	0.60	0.42
LWP								1	0.85	0.96	0.98	0.83
UEP									1	0.95	0.88	0.63
MEP										1	0.96	0.74
LEP											1	0.85
LSR												1

allowing for a meaningful breakdown of the expected upper and lower estuarine classes. The classification algorithm was allowed to generate starting vectors diagonally along the n-dimensional histogram of the entire data set (limited to the classification area). The analysis led to the formation of several large cohesive classes and a few small scattered classes, mainly composed of edge pixels. These extra classes needed to be accepted for the sake of improving the classification of the actual area of interest. When the minimum change threshold was reached, the program converged and all pixels were classified using the last set of class vectors.

To test if the specific selection of the eight scenes had a direct effect on the resulting classes, several tests of the approach were performed using different combinations of eight scenes from among the 14 available, while maintaining a seasonal spread in the dates, as well as using all scenes that were free of atmospheric interference or ice. As expected, there were minor differences among these solutions. However, the gross characteristics of the most important six classes did not change in these tests.

Results

The general patterns observed in the seasonal temperature signals of the classes identified by both the regional and unsupervised classification analyses are intuitive, controlled primarily by surface to volume ratios of the respective regions (Table 2) and modified to some extent by tidal exchange among the regions. Estuarine regions lose more heat proportionately than the ocean during the winter and gain more heat during the summer. Lakes exhibit an extreme of this behaviour, as they are generally the warmest bodies

during the summer and coldest during the winter. The ocean temperature is obviously much more moderate, due to the relatively vast volume of these regions.

Although these general results are not at all surprising, they provide the critical context for assessing the spatial extent, thermal magnitude and temporal character of the effects of thermal effluent from the BPPs. In order to apply a Space for Time Substitution, it is critical to establish that the physical properties of the region selected to be the control are indeed functionally comparable to the impacted site. As presented in Table 2, Upper Narragansett Bay is the region that most closely matches the physical and functional properties of Mount Hope Bay. Employing both deductive (regional classification) and inductive (unsupervised classification) methods to the satellite data, the same basic conclusion is reached; the thermal properties of Mount Hope Bay are unique, with relatively greater temperatures in the summer and autumn than the control sites. These results are discussed in detail below.

Regional classification

The seasonal surface temperature signals of the twelve Narragansett Bay areas relative to the Narragansett Bay mean exhibited three different patterns (Figure 6). The upper estuarine regions were generally warmer than the bay average during the summer and cooler during the winter, whereas the lower estuarine regions had the opposite behaviour, and intermediate regions had damped temperature signals relative to the estuary mean. Correlation coefficients among the 12 seasonal temperature signals provide a statistical basis for the breakdown of the estuary into these three groups (Table 3). Significant

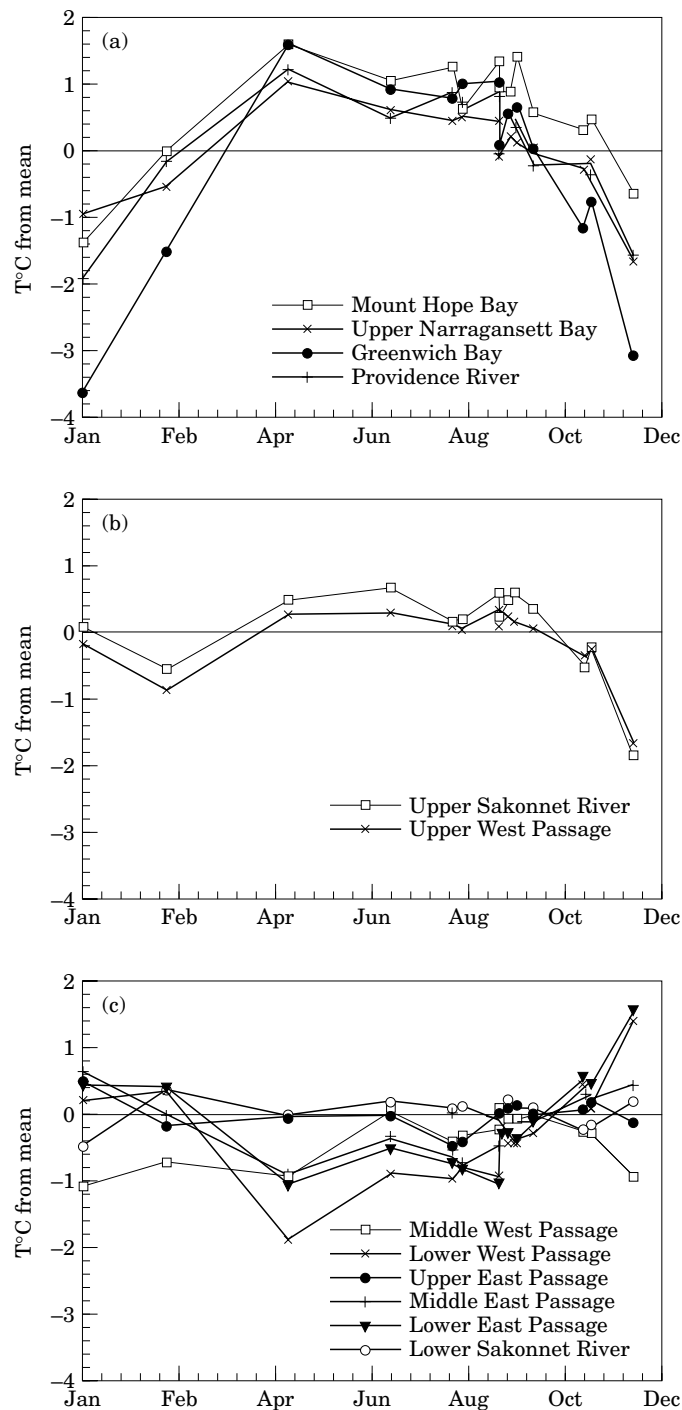


FIGURE 6. Seasonal temperature signals for the 12 study areas used in the regional classification, separated into the three main groups defined in Table 3. All temperatures are the difference in temperature from the mean of all twelve regions. Negative values are colder than the mean and positive are greater than the mean.

correlations ($r > 0.6$) existed among the members of each group (although each area was not necessarily correlated with every other area within its group) and only negative or insignificant correlations existed between areas of different groups.

The seasonal temperature signals of the 12 predefined study areas provide the opportunity to relate thermal properties to the known physical characteristics of each area. In the lower estuary, the Lower East Passage and Lower West Passage exhibited the

TABLE 4. Area covered by specific classes from the unsupervised classification

	Lakes	Greenwich Bay	Upper Estuary	Mount Hope Bay	Lower Estuary	Oceanic
Number of pixels	4625	6635	36 227	10 127	18 290	115 520
Area (km ²)	16.6	23.8	130.4	36.5	65.8	415.9

most extreme thermal behaviour relative to the Narragansett Bay mean, as they are most influenced by advective exchange between the estuary and oceanic waters. The strength of oceanic influence in the East Passage is reflected by the facts that the entire East Passage was classified as lower estuarine and that the lower East Passage exhibited the strongest 'oceanic' signal [Figure 6(c)]. It is known that on a rising tide, most of the oceanic water enters the estuary through the East Passage, which is the deepest part of the system (Kremmer & Nixon, 1978). The Upper West Passage and Upper Sakonnet River formed a transitional group, characterized as a zone of mixing between waters which are more influenced by shallow water processes and those which are more tidally influenced [Figure 6(b)].

The character of the regions within the upper estuarine group were more strongly dependent upon the varying physical characteristics among the areas [Figure 6(a)]. For example, Greenwich Bay is shallow with a theoretically high tidal flushing rate and low freshwater input; its seasonal temperature signal was fairly extreme in comparison to the other upper estuarine areas. Greenwich Bay's high surface area to volume relationship is the most important factor determining its thermal behaviour. Though the high predicted tidal flushing (the highest among all areas, Table 2) would tend to counter the effect of the surface to volume ratio and thus the seasonal temperature fluctuations, studies have shown that there is much less tidal exchange than expected due to the specific geographic characteristics. The other three upper estuarine areas all have smaller surface area to volume ratios and weaker seasonal temperature signals. In comparison, the freshwater lakes, which are shallow and isolated, have even stronger signals than Greenwich Bay. These relationships suggest that regional surface to volume ratio is the most important factor in determining thermal characteristics in the upper estuary.

Of all the regions of Narragansett Bay characterized by Kremmer and Nixon (1978), Upper Narragansett Bay and Mount Hope Bay are the most similar on the basis of physical properties and location relative to important tidal exchanges with the coastal ocean

(Table 2). The two areas are about the same size and their surface area to volume ratios are nearly identical. Upper Narragansett Bay flushing times are slightly faster, but are in the same general range as those for Mount Hope Bay. In a natural system, it would be expected that regions with similar physical characteristics would have comparable seasonal temperature characteristics. Thus, based upon its similar size, shape, and physical forcing, Upper Narragansett Bay serves as an appropriate area for comparison to Mount Hope Bay and its thermal characteristics in a Space for Time Substitution impact assessment.

The seasonal temperature characteristics of Mount Hope Bay and Upper Narragansett Bay were somewhat correlated during the winter months, but Mount Hope Bay failed to cool down at the rate of Upper Narragansett Bay through the fall [Figure 6(a)]. *t*-tests between Upper Narragansett Bay and Mount Hope Bay proved their mean temperatures to be significantly different during the summer-fall period, during which time Mount Hope Bay had a mean temperature 0.8 °C warmer than Upper Narragansett Bay. Greenwich Bay, the Providence River and Upper Narragansett Bay all became cooler than the Narragansett Bay mean by early October, yet Mount Hope Bay was only colder than the bay mean in one January scene.

Unsupervised classification

The selected water area was successfully divided into six different classes, based upon seasonal surface temperature signals (Figure 7). The classes consisted of freshwater lakes, the ocean, the upper estuary, the lower estuary, Greenwich Bay and Mount Hope Bay, and the total area covered by each class is given in Table 4. Four additional classes were generated, mainly consisting of pixels at the boundaries between land and water (not shown). These classes were all small and their behaviour was probably affected by the presence of land in some of the pixels, so they were not considered further in the analysis.

In general, the freshwater lakes exhibited the strongest seasonal temperature signal relative to the estuary mean: they were very warm during the

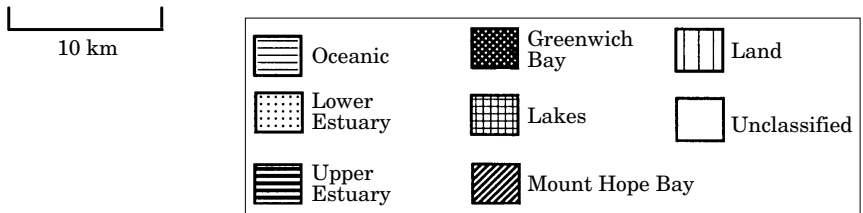
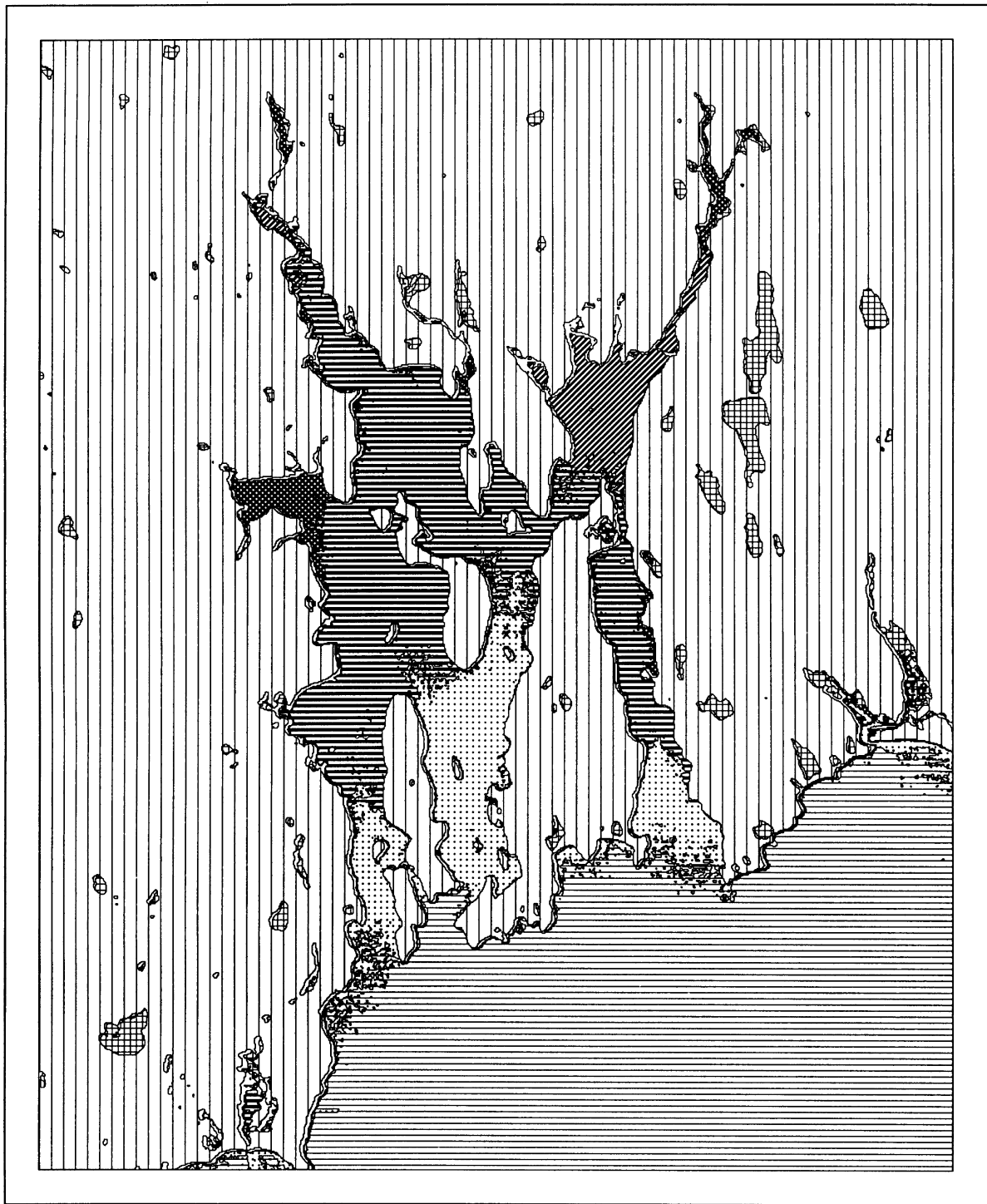


FIGURE 7. Results of the unsupervised classification. Each of the six major classes represents areas with common seasonal temperature signatures. Note that the Mount Hope Bay class is unique spatially, largely confined to Mount Hope Bay, with a minor grouping in the upper Providence River.

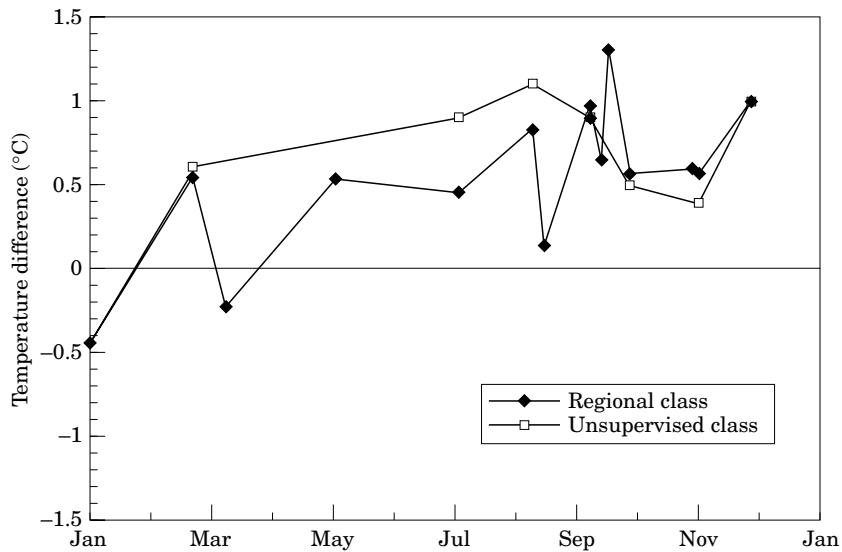


FIGURE 8 Magnitude of the Mount Hope Bay temperature anomaly from both the regional and unsupervised classifications. These are the anomalies between the Mount Hope Bay class and the class containing Upper Narragansett Bay.

summer months and very cold during the winter. Greenwich Bay behaved similarly, only to a lesser degree. The upper estuary was the largest class (Table 4), and therefore provided the greatest contribution toward the mean value for each scene. Thus, the upper estuary temperature signal relative to the mean was fairly weak. The ocean was significantly warmer than the study area mean during the winter and colder during the summer, as would be expected, and the lower estuary exhibited temperatures transitional between the ocean and the upper estuary.

Mount Hope Bay exhibited a unique temperature behaviour, as it was on average 0.8 °C warmer than the rest of the upper estuary over the range of scenes analysed (Figure 8). Unlike Greenwich Bay, which was relatively warm during the summer and cold during the winter, or the lower estuary which behaved in an opposite manner, Mount Hope Bay was consistently warm, only dropping below the estuary-wide average in November, at which point it was still warmer than the rest of the upper estuary.

One of the strengths of the unsupervised classification is that patterns of seasonal thermal behaviour are objectively mapped. Almost without exception, a consistent sequence of seasonal thermal behaviours are observed moving from the buffered signals of the coastal ocean, through the transitional and dominant estuary regions to the shallow estuary and lakes. This can be observed in Figure 7 through to the highest reaches of Narragansett Bay as well as smaller inlets along the coast. This general pattern, however, is interrupted in Mount Hope Bay, with a small cluster of similar seasonal properties on the west side of the

Providence River. Significantly, this correlates with the location of the Manchester Street Power Plant which discharges a relatively small volume of thermal effluent.

Discussion

The most striking behaviour among the four upper estuarine signals in the regional classification is that Mount Hope Bay fails to cool from mid-summer through autumn in comparison to the Narragansett Bay mean (Figure 6). These anomalously warm temperatures cannot be explained by simple physical characteristics. If anything, Mount Hope Bay's slightly slower tidal flushing rate in comparison to the other upper estuarine areas (Table 2) would theoretically cause a stronger cooling affect during the autumn. The unique behaviour of Mount Hope Bay is highlighted by the fact that the bay comprises its own class in the unsupervised classification. Mount Hope Bay is not distinctively shallow or isolated from tidal waters, in fact it has very similar physical characteristics to the rest of upper Narragansett Bay. In addition, there are no natural physical parameters which would cause a water body to remain anomalously warm year-round.

Seasonal temperature patterns in the estuary are a direct result of radiant heat exchange at the surface and advective exchange with oceanic waters. Both processes are seasonal in nature, such that heat is gained through the surface during the summer (lost during the winter) and gained from relatively warm tidal waters during the winter (lost during the

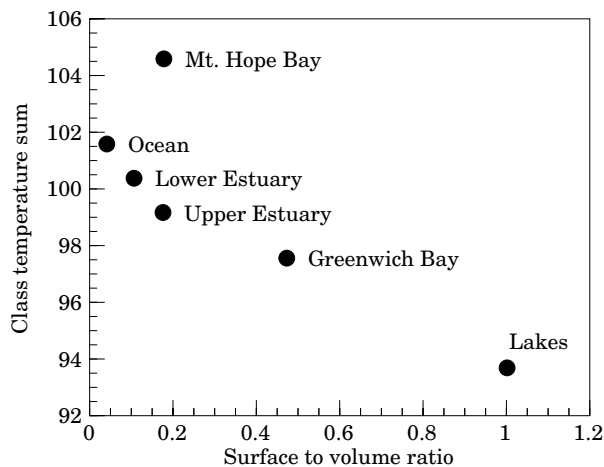


FIGURE 9. Relationship between the surface to volume ratio for each region and the integrated temperature across the scenes used in the regional classification. All the regions follow a monotonic relationship except for Mount Hope Bay.

summer). The seasonal temperature signal of a particular area is a direct reflection of the balance between these processes, which in this region is a function of surface area to volume ratio first and advective exchange second. The upper estuary reflects a fairly level balance of these processes measured relative to the study area mean.

Mount Hope Bay, however, exhibits temperatures that are anomalous for the patterns of seasonal temperatures determined through this analysis. This is illustrated most succinctly in Figure 9. The seasonal temperature signatures derived from the unsupervised classification were summed over the eight scenes to produce a single number. When plotted against the surface to volume ratio, there is a clear trend from low values for high ratios and high values for low ratios. Mount Hope Bay, however, departs significantly from this trend.

Excess summer warming relative to Upper Narragansett Bay could result from the shallow average depth of Mount Hope Bay. However, this hypothesis predicts that the bay should also lose proportionately more heat during the winter, which is not evidence in these data. Alternatively, we could explain relatively warm temperatures during the winter with a potentially large tidal influence, but this would similarly lead to cooler temperatures during the summer. Again, there is no evidence to support this hypothesis through either our understanding of the physical character of the bay or the analysis of the satellite data.

On average, Mount Hope Bay was typically 1 °C warmer than the upper estuarine class. Major

alterations to the system's heat budget are required to create an anomaly with the spatial extent and temporal consistency of this feature. The simplest and most likely explanation for the relatively warm year-round temperatures in Mount Hope Bay is the constant discharge of thermal effluent into the bay by the Brayton Point Power Station. The excess heat load is the only plausible explanation for the consistently warm temperatures in the bay. The extent of the Mount Hope Bay class (Figure 7), is an indication of the boundaries of the area which was consistently affected by constant warming. This thermally anomalous area covers an area of approximately 35 km² (Table 4).

Unsupervised classification also facilitated the recognition of smaller scale patterns which were averaged out by the regional approach. For example, there was an identifiable trace of the 'Mount Hope Bay' class in the upper Providence River, near the location of the Manchester Street Power Plant (Figure 7). Although the thermal affects of this plant were not as visible in the satellite images as the plume from the larger Brayton Point Station in Mount Hope Bay, the fact that water in the upper Providence River exhibited similar seasonal behaviour to that of Mount Hope Bay (the temperature of which is known to be driven by the influence of thermal effluent) suggests that the Manchester St. Plant may after all have an identifiable effect on the thermal properties of adjacent waters. This potential effect does however occur on a much smaller scale than the apparent influence of BPPS on Mount Hope Bay.

The almost year-round persistence of a decreasing temperature gradient with distance from the Brayton Point Power Station in Mount Hope Bay suggests that the plant's thermal effluent constantly drives the distribution of heat within the bay. The persistent temperature gradient and the extent of the Mount Hope Bay class in the unsupervised classification both suggest that the influence of the plant's thermal effluent is widespread throughout the bay and is not an isolated feature.

Conclusions

Characterization of the extent of impact from effluent can be a challenging problem, and one that needs to take into consideration multiple potential physical factors in addition to the hypothesized anthropogenic factor. Commonly it is not possible to use before-after comparison techniques due to the lack of adequate data. This is particularly true for estuarine environments where the complex relationships between physical properties and processes place large

constraints on the density and frequency of observations required to test any impact hypothesis. A space for time substitution approach can be exploited where, again, sufficient data exists. In this analysis, it has been demonstrated that remotely sensed data have several unique properties that lend themselves to impact assessments. In particular, the wide areal coverage, instantaneous acquisition, imaging format and fine-scale resolution are ideally suited to establish the physical and spatial properties of impacted areas using a space for time substitution approach.

Remotely sensed thermal data provided a unique tool to develop an understanding of seasonal and spatial temperature dynamics in Narragansett Bay and the relationships between temperature and physical forcing factors. By establishing these key relationships, it was then possible to establish that the thermal properties of Mount Hope Bay were anomalous, and to quantify the spatial extent and magnitude of the anomaly. These questions could not have been adequately addressed by conventional methods or *in situ* data.

Both approaches used to classify Narragansett Bay in terms of seasonal temperature behaviour resulted in similar descriptions of the estuary's thermal properties, which included the intuitive characteristic behaviour of the ocean, the lower estuary, the upper estuary and the inland water bodies. Pre-defined study areas allowed us to consider the thermal properties of each area in the context of its physical character, emphasizing the importance of surface area to volume relationships in the upper estuary, and circulation patterns in the lower estuary. The unsupervised approach provided an unbiased classification of functionally similar systems in Narragansett Bay, identifying boundaries among areas with different seasonal temperature signals. Mount Hope Bay behaved anomalously in the context of both analyses and was particularly warm during late summer months, corresponding to the time of maximum heat output from the plant.

The detailed description of large-scale seasonal dynamics in Mount Hope Bay provided here sheds light on the previously uncertain influence of the Brayton Point Power Station on the thermal characteristics of Mount Hope Bay. This analysis shows that the temperature of Mount Hope Bay is on average 0.8 °C warmer than comparable regions elsewhere in Narragansett Bay, with an affected area of 35 km². Because this is an averaged effect, there are regions within the affected area that consistently experience higher temperatures. An understanding of the thermal processes at work is but one component of a solution to the problem of depleted fisheries in the bay. Although it is fairly well-accepted that the decline in

fisheries was in some way linked to the 1985 changes in the operations of the plant, there are numerous mechanisms by which the plant could impact fish populations, including impingement, entrainment, chlorination and depletion of dissolved oxygen, as well as temperature effects. Therefore, in addition to a description of the physical character of Mount Hope bay, a more detailed picture of the bay's ecosystem dynamics is vital to the full consideration of this issue.

Acknowledgements

The project has benefited tremendously from interactions and discussions with a great many people including Chris Deacutis, Warren Prell, Steven Hamburg, Craig Swanson, Dan Mendehelson, John Torgan and members of the New England Power technical staff. Support from the Rhode Island Department of Environmental Management (Aqua Fund, AQF-36) for acquisition of the Landsat data is gratefully acknowledged as well as support from the NASA Commercial Remote Sensing Program office (NAG13-39).

References

- Avery, T. E. & Berlin, G. L. 1992 *Fundamentals of Remote Sensing and Airphoto Interpretation*, 5th Ed. Prentice Hall, Upper Saddle River, NJ.
- Chinman, R. A. & Nixon, S. W. 1985 Depth-Area-Volume Relationships in Narragansett Bay. Graduate School of Oceanography, the University of Rhode Island. *NOAA/Sea Grant Marine Technical Report 87*.
- Dixon, A. M., Karp, C. & Penniman, C. 1991 Mount Hope Bay Briefing Paper and Proceedings from Narragansett Bay Project Management Committee. *Narragansett Bay Project Report 91-65*.
- Foody, G. M., Campbell, N. A., Trood, N. M. & Wood, T. F. 1992 Derivation and applications of probabilistic measures of class membership from the maximum-likelihood classification. *Photogrammetric Engineering and Remote Sensing* **58**, 1335-1341.
- Gibbons, D. E., Wukelic, G. E., Leighton, J. P. & Doyle, M. J. 1989 Application of Landsat Thematic Mapper Data for Coastal Thermal Plume Analysis at Diablo Canyon. *Photogrammetric Engineering and Remote Sensing* **55**, 903-90.
- Gibson, M. R. 1996 Comparison of Trends in the Finfish Assemblage of Mt. Hope Bay and Narragansett Bay in Relation to Operations at the New England Power Brayton Point Station. *RI Division Fish and Wildlife Research Reference Document 995/1*.
- Hamburg, S. P. 1984 *Organic matter and nitrogen accumulation during 70 years of old-field succession in central New Hampshire*. Ph.D. Thesis, Yale University, 278 pp.
- Hargrove, W. W. & Pickering, J. 1992 Pseudoreplication: A sine Qua non for regional ecology. *Landscape Ecology* **6**, 251-258.
- Hurlbuert, S. H. 1984 Pseudoreplication and the design of ecological field experiments. *Ecological Monographs* **54**, 187-211.
- Jahne, B. 1991 *Digital Image Processing*. Springer-Verlag, New York, 250 pp.
- Jain, A. K. 1989 *Fundamentals of Digital Image Processing*. Prentice Hall, New Jersey, 500 pp.
- Jeffries, H. P. 1994 The impacts of warming climate on fish populations. *Maritimes* **37**, 12-15.
- Jensen, J. R. 1996 *Introductory Digital Image Processing: A Remote Sensing Perspective*. Simon and Schuster, New Jersey, 316 pp.

- Kremer, J. N. & Nixon, S. W. 1978 *A Coastal Marine Ecosystem*. Springer-Verlag, New York, Berlin, Heidelberg.
- Lin, P. & Regier, H. A. 1995 Use of Arrhenius models to describe temperature dependence of organismal rates in fish. In *Climate Change in Northern Fish Populations* (Beamish, R. J., ed.). *Canadian Special Publication of Aquatic Science*, 121 pp.
- Paine, R. T. 1993 A Salty and Salutary Perspective on Global change. In *Biotic Interactions and Global Change* (Kareiva, P. M., Kingsolver, J. G. & Huey, R. B., eds). Sinauer Assoc, Sunderland, MA.
- Sabins, M. J. 1987 Convergence and consistency of fuzzy c-Means/ISODATA algorithms. *IEEE Transactions Pattern and Machine Intelligence* **9**, 661–688.
- Schneider, K & Mauser, W. 1996 Processing and Accuracy of Landsat Thematic Mapper Data for Lake Surface Temperature Measurement. *International Journal of Remote Sensing* **17**, 2027–2041.
- Spaulding, M. L., White, F. M., Heinmiller, P., Simoneau, M. M., Liang, S. J., & Choi, J. K. 1988 Circulation Dynamics in Mount Hope Bay and the Lower Taunton River. *Narragansett Bay Project Report 88-12*.
- Stewart-Oaten, W., Murdoch, W. W. & Parker, K. R. 1986 Environmental impact assessment: “Pseudoreplication” in time? *Ecology* **67**, 929–940.
- Tissot, B. N., Lubchenco, J. & Navarrette, S. 1991 Effects of Global Warming on Coastal Marine Ecosystems: Implications of thermal discharge studies. *Bulletin of the Ecological Society America* **72**, 268.
- Tou, J. T. & Gonzalez, R. C. 1997 *Pattern Recognition Principles*. Addison-Wesley, Massachusetts, 277 pp.
- Underwood, A. J. 1993 The mechanics of spatially replicated sampling programmes to detect environmental impacts in a variable world. *Australian Journal of Ecology* **18**, 99–116.
- Valiela, I. 1995 *Marine Ecological Processes*. Springer, New York.
- Yokoyama, R., Tanba, S. & Souma, T. 1995 Sea surface effects on the sea surface temperature estimation by remote sensing. *International Journal of Remote Sensing* **16**, 227–238.